

# Hadron wave functions and the issue of nucleon deformation \*

C. Alexandrou<sup>a</sup>, Ph. de Forcrand<sup>b</sup> and A. Tsapalis<sup>a</sup>

<sup>a</sup>Department of Physics, University of Cyprus, CY-1678 Nicosia, Cyprus

<sup>b</sup>ETH-Zürich, CH-8093 Zürich and CERN, CH-1211 Geneva 23, Switzerland

Using gauge invariant hadronic two- and three- density correlators we extract information on the spatial distributions of quarks in hadrons, and on hadron shape and multipole moments within quenched lattice QCD. Combined with the calculation of N to  $\Delta$  transition amplitudes the issue of nucleon deformation can be addressed.

## 1. Introduction

Correlation functions calculated in lattice QCD can be connected to basic hadronic features. Two- and three- density correlators for mesons and baryons reduce in the non-relativistic limit to the square of the wave function and therefore provide detailed information on hadron structure such as quark spatial distributions, hadronic shapes and charge radii. In addition lattice results can be used to test predictions in various models. Direct connection to the issue of nucleon deformation, currently under experimental investigation [1,2], is made by calculating the  $\gamma^*N$  to  $\Delta$  transition form factors in quenched and unquenched lattice QCD. The aim is to obtain an accurate determination of the ratio of the electric quadrupole to the magnetic dipole amplitudes,  $R_{EM}(q^2)$ , as a function of the momentum transfer  $q$ . A non-zero  $R_{EM}$  arises due to deformation in the nucleon and/or  $\Delta$  and it is attributed to different mechanisms in the various models: in quark models the deformation arises due to the colour-magnetic tensor force whereas in 'cloudy' baryon models due to the meson exchange currents.

Let us first consider the equal-time correlators [3],

$$C_{\Gamma}^H(\mathbf{r}, t) = \int d^3r' \langle H | \hat{\rho}_{\Gamma}^u(\mathbf{r}', t) \hat{\rho}_{\Gamma}^d(\mathbf{r}' + \mathbf{r}, t) | H \rangle \quad , \quad (1)$$

with  $\hat{\rho}_{\Gamma}^u(\mathbf{r}, t)$  given by the normal order product :  $\bar{u}(\mathbf{r}, t)\Gamma u(\mathbf{r}, t)$  :. For  $\Gamma = \gamma_0$  and  $\Gamma = \mathbf{1}$  we obtain, in the nonrelativistic limit, the charge and matter density respectively. For  $\Gamma = \gamma_5$  we obtain the pseudoscalar density which we will compare to bag model predictions. The matrix elements of two-density correlators are shown schematically in Fig. 1. The advantage of using density correlators is that they are gauge-invariant unlike Bethe-Salpeter amplitudes. For baryon wave functions three-density correlators are needed. Here we will only show results for the one-particle density obtained after integrating the wave function over one relative distance. The diagram involved is shown in the lower part of Fig. 1.

Since the spectroscopic quadrupole moment of the nucleon vanishes in order to determine any possible deformation we evaluate the N to  $\Delta$  electromagnetic transition form

---

\*Talk presented by C. Alexandrou.

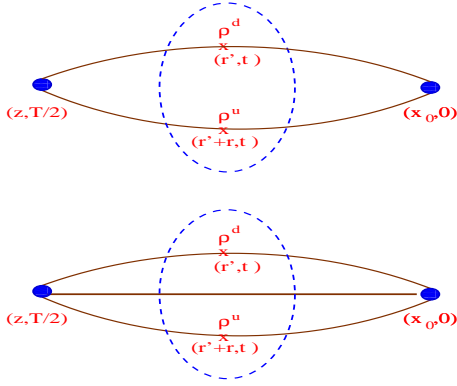


Figure 1. Equal-time correlator for a meson (upper) and a baryon (lower).

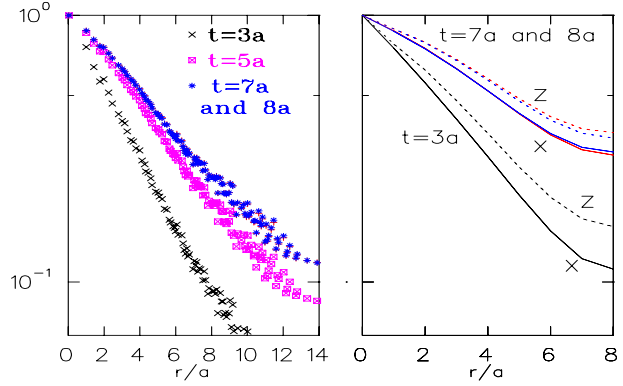


Figure 2. Time evolution to ground state for the rho meson at  $\kappa = 0.153$ .

factors. We calculate the three-point correlation functions [4]  $\langle G_\sigma^{\Delta j^\mu N}(t_2, t; \mathbf{p}', \mathbf{p}; \Gamma) \rangle$  and  $\langle G_\sigma^{N j^\mu \Delta}(t_2, t; \mathbf{p}', \mathbf{p}; \Gamma) \rangle$  and consider the following ratio [5]

$$R_\sigma(t_2, t; \mathbf{p}', \mathbf{p}; \Gamma; \mu) = \left[ \frac{\langle G_\sigma^{\Delta j^\mu N}(t_2, t; \mathbf{p}', \mathbf{p}; \Gamma) \rangle \langle G_\sigma^{N j^\mu \Delta}(t_2, t; -\mathbf{p}, -\mathbf{p}'; \Gamma^\dagger) \rangle}{\langle -g_{ij} G_{ij}^{\Delta \Delta}(t_2, \mathbf{p}'; \Gamma_4) \rangle \langle G^{NN}(t_2, -\mathbf{p}; \Gamma_4) \rangle} \right]^{1/2}$$

$$t_2 - t \gg 1, t \gg 1 \quad \left( \frac{E_N(\mathbf{p}) + M_N}{2E_N(\mathbf{p})} \right)^{1/2} \left( \frac{E'_\Delta(\mathbf{p}') + M_N}{2E'_\Delta(\mathbf{p}')} \right)^{1/2} \bar{R}_\sigma(\mathbf{p}', \mathbf{p}; \Gamma; \mu) \quad (2)$$

from which the transition form factors can be extracted. The index  $\sigma$  is the Lorentz index for a spin- $\frac{3}{2}$  field,  $j^\mu(x)$ , is the lattice conserved electromagnetic current inserted at time  $t$ ,  $E_N(\mathbf{p})$  and  $E'_\Delta(\mathbf{p}')$  are the energies of the nucleon and the  $\Delta$  respectively and  $t_2$ , the time location of the sink, is varied to identify the ground state. We use projection matrices  $\Gamma_j = 1/2 \begin{pmatrix} \sigma_j & 0 \\ 0 & 0 \end{pmatrix}$  and  $\Gamma_0 = 1/2 \begin{pmatrix} I & 0 \\ 0 & 0 \end{pmatrix}$  as in ref. [5].

## 2. Results

We have analysed 220 quenched configurations at  $\beta = 6.0$  for a lattice of size  $16^3 \times 32$  at  $\kappa = 0.15, 0.153, 0.154, 0.155$  which give ratio of pion to rho mass of 0.88, 0.84, 0.78, 0.70 respectively. Using the standard definition of the naive quark mass,  $2m_q a = (1/\kappa - 1/\kappa_c)$ , where  $\kappa_c$  is the value of  $\kappa$  at which the pion becomes massless, we find  $m_q \sim 300, 170, 130$  and 85 MeV respectively. We used the value of the string tension to set the physical scale obtaining for the inverse lattice spacing  $a^{-1} \sim 1.94$  GeV. The density insertions are taken at  $t = T/4 = 8a$ . To check that this time interval is long enough to extract the physical hadronic ground state we computed the density-density correlators for varying values of the insertion time  $t$ . Fig. 2 shows the results for the rho correlators which converge when  $t > 6a$ . Moreover, we note a clear deformation (ratio  $C_{\gamma_0}^\rho(x, 0, 0)/C_{\gamma_0}^\rho(0, 0, z) \neq 1$ ) which remains approximately the same as early as  $t = 3a$  even though the  $z$ - and  $x$ -profiles change appreciably showing that the deformation is a robust, physical property of the rho meson in its ground state as well as its low-lying excited states.

The dependence of hadron wave functions on the quark mass is displayed in Fig. 3 where we plot the density-density correlators at various  $\kappa$  values for the pion, the rho, the nucleon and the  $\Delta^+$  normalized to unity. The size of the nucleon and  $\Delta$  wave functions do not change for naive quark mass smaller than 130 MeV. The rho wave function shows the largest variation with the quark mass. In Fig.4 we compare the matter and charge densities at  $\kappa = 0.153$ . We find that the matter density falls off more rapidly than the charge density and it has the same shape for all four hadrons.

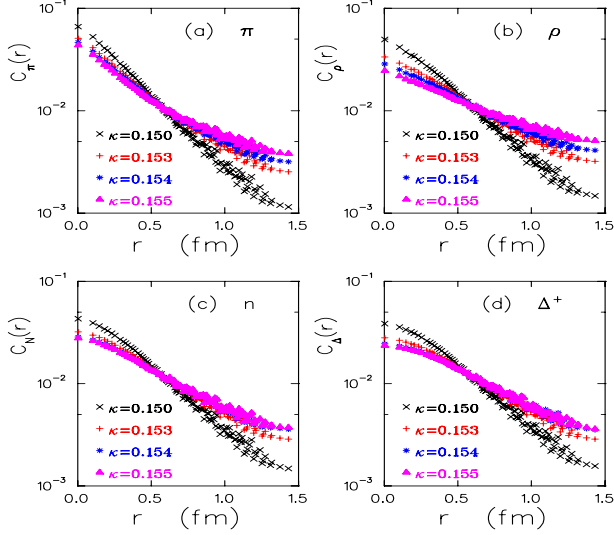


Figure 3. Density-density correlators as a function of the quark mass.

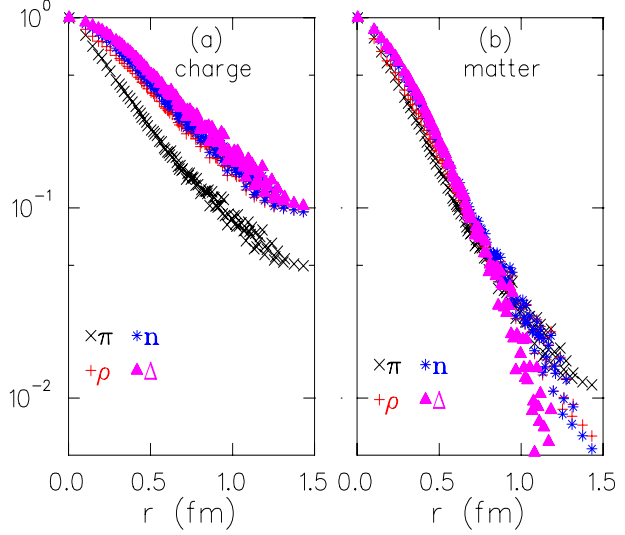


Figure 4. Comparison of charge (a) and matter (b) densities at  $\kappa = 0.153$ .

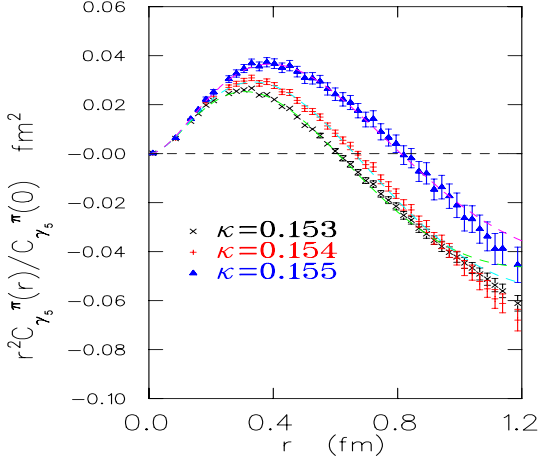


Figure 5. The pseudoscalar density for the pion at  $\kappa = 0.153, 0.154$  and  $0.155$  with fits to  $r^2(a + br^2 + cr^4) \exp(-mr)$ .

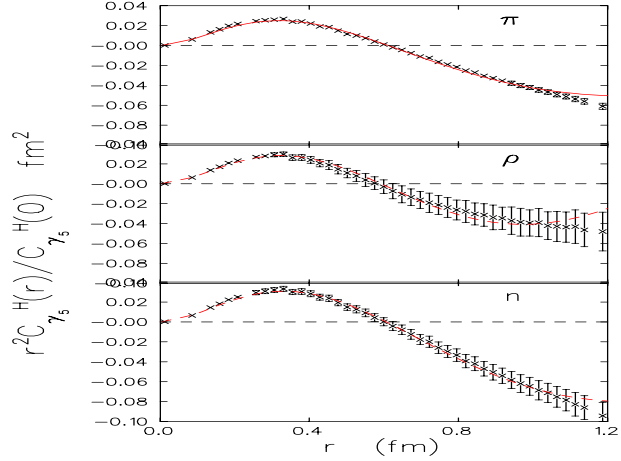


Figure 6. Pseudoscalar density for the pion (upper), the rho (middle) and the nucleon (lower) at  $\kappa = 0.153$ . Fits as in Fig. 5.

The pseudoscalar density for the pion is shown in Fig. 5 for  $m_\pi/m_\rho = 0.84, 0.78$  and  $0.70$ . In Fig. 6 it is compared with that for the rho and the nucleon at  $m_\pi/m_\rho = 0.84$ . The bag model predicts that the integral  $\int d^3r C_{\gamma_5}^H(r)$  is zero [6]. A reasonable fit is obtained by an exponential times a polynomial ansatz. The long tail of the data and the integral of the fitted ansatz both favor a non-zero integral. However a careful extrapolation to the continuum limit (using large volumes) is required for this quantity, especially with Wilson fermions as used here.

The rho deformation seen in Fig. 2 can be made more quantitative by analysing the density-density correlator into a dominant  $L = 0$  state and a suppressed  $L = 2$  [7]:

$$\langle \rho_j(\mathbf{0}) | \hat{\rho}_{\gamma_0}(\mathbf{r}) \hat{\rho}_{\gamma_0}(\mathbf{0}) | \rho_j(\mathbf{0}) \rangle = \phi_1(r) + \frac{(3x_j^2 - r^2)}{3r^2} \phi_2(r) \quad (3)$$

where  $|\rho_j(\mathbf{0})\rangle$  is a zero momentum state with polarization  $j$ .

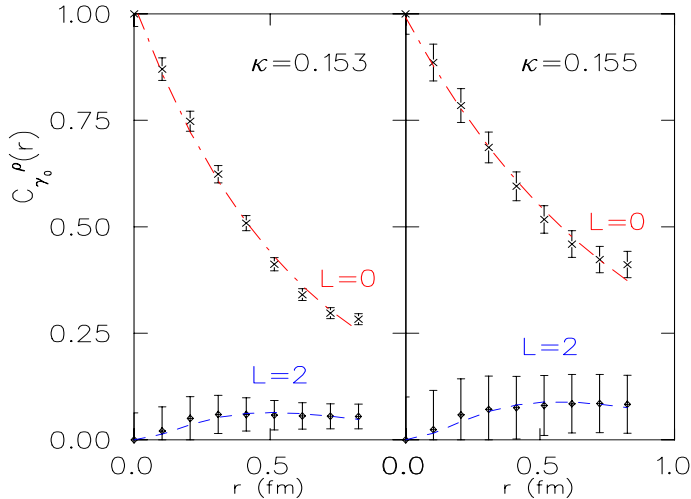


Figure 7. Decomposition of  $C_{\gamma_0}$  for the rho into angular momentum part  $L = 0$  and  $L = 2$ .

First lattice results for the ratio of the electric quadrupole to magnetic dipole amplitudes,  $R_{EM}$ , for both quenched and for two dynamical Wilson fermions are obtained at the smallest allowed lattice momentum,  $\mathbf{q} = (2\pi/L_s, 0, 0)$ , where  $L_s$  is the spatial length of the lattice. At  $\mathbf{q}^2 = 0.54 \text{ GeV}^2$  for the unquenched theory using the SESAM configurations [8] we find in the chiral limit  $R_{EM} \sim (-3.7 \pm 0.5)\%$ . For  $\mathbf{q}^2 = 0.15 \text{ GeV}^2$  in the quenched theory on a lattice of size  $32^3 \times 64$  at  $\beta = 6.0$  we find  $R_{EM} \sim (-3.0 \pm 0.3)\%$ . We used the nucleon mass to set the physical scale. Finite lattice spacing effects on the  $R_{EM}$  ratio can be significant and are currently under investigation. The finite volume dependence on  $R_{EM}$  is also under study.

### 3. Conclusions

We have presented a gauge-invariant determination of hadron profiles in the quenched approximation. We have found that the rho wave function shows the strongest dependence on the quark mass whereas the nucleon and  $\Delta$  the weakest. We have established that the rho is deformed with deformation which increases as we approach the chiral limit, whereas the  $\Delta^+$  has no statistically significant deformation. The matter density is similar for all four hadrons and falls off more rapidly than the charge density. Using state-of-the-art lattice techniques the phenomenologically important  $R_{EM}$  has been extracted for two  $q^2$  values and found to be consistent with experimental measurements.

### REFERENCES

1. C. Mertz *et al.*, Phys. Rev. Lett. **86** (2001) 2963
2. K. Joo *et al.*, Phys. Rev. Lett. **88** (2002) 122001.
3. C. Alexandrou, Ph. de Forcrand and A. Tsapalis, Phys. Rev. D **66** (2002) 094503; Nucl. Phys. B (Proc. Suppl.) **119** (2003) 422.
4. C. Alexandrou *et al.*, in preparation; hep-lat/0209074.
5. D. B. Leinweber, T. Draper and R. M. Woloshyn, Phys. Rev. D **48** (1993) 2230.
6. M. Lissia, M.-C. Chu, J. W. Negele and J. M. Grandy, Nucl. Phys. A **555** (1993) 272.
7. R. Gupta, D. Daniel and J. Grandy, Phys. Rev. D **48** (1993) 3330.
8. N. Eicker *et al.*, Phys. Rev. D **59** (1999) 014509.

As shown in Fig. 7, a good description of the rho correlator, is obtained by taking  $\phi_1(r) = A \exp(-m_1 r)$  and  $\phi_2(r) = B r^2 \exp(-m_2 r)$ . Using the values extracted from the fits and neglecting  $B^2$  terms we find for the deformation  $\delta \equiv (3/4)(\langle 3z^2 - r^2 \rangle / \langle r^2 \rangle) \sim 0.01$  with an error of about 80% which mainly arises from the poor determination of the coefficient of the  $L = 2$  state. A direct determination of the quadrupole moment from the rho correlator yields  $\delta = 0.03 \pm 0.01$  in reasonable agreement with the value obtained from the angular decomposition.